communications earth & environment

ARTICLE

https://doi.org/10.1038/s43247-022-00549-9 OPEN

# Earthquakes control the impulsive nature of crustal helium degassing to the atmosphere

Antonio Caracausi [1✉], Dario Buttitta[1,4], Matteo Picozzi[2], Michele Paternoster [1,4] & Tony Alfredo Stabile [3]

Deep fluids play active roles during the preparatory phases of large earthquakes and, through their chemical signature, carry information about deep processes within the seismogenic crust. Due to its inertness and isotopic signature, helium (the lightest noble gas) is a useful tracer for investigating the processes of storage and transfer of fluids through the crust, including those prior to hazardous earthquakes. Here we analyse a 12-year earthquake catalogue from the Irpinia Fault Zone, Italy, to compute the $^4$He outputs from the seismogenetic fault zones (from $10^4$ to $10^6$ mol $y^{-1}$ with an annual tenfold variability) and compare these with estimates of long-term helium flux. We find that low-magnitude earthquakes ($M < 4$) efficiently contribute to variations of the crustal helium output into the atmosphere which supports the impulsive nature of He degassing in tectonically active continental regions. We conclude that there is a quantitative relationship between crustal helium outputs and the volume of fault zones, and suggest variations in helium flux may represent a gauge of changes in the stress field that are related to the nucleation of earthquakes.

[1] Istituto Nazionale di Geofisica e Vulcanologia, Sezione di Palermo, Palermo, Italy. [2] University of Naples Federico II, Naples, Italy. [3] Istituto di Metodologie per l'Analisi Ambientale (IMAA, CNR), Potenza, Italy. [4] Present address: University of Basilicata, Potenza, Italy. ✉email: antonio.caracausi@ingv.it



Content courtesy of Springer Nature, terms of use apply. Rights reserved

The composition of the atmosphere and its evolution over time was mainly driven by natural degassing from the Earth interior[1] up to the industrial age. Volcanic activity fed the release of huge amounts of volatiles into atmosphere[2], making volcanoes major emitters of natural volatiles and hence controlling the budget of volatiles in the atmosphere. Considerable attention has recently been paid to the outgassing in active tectonic regions because faults are regions of enhanced permeability and porosity where fluids can migrate through the whole crust[3,4], and these latter can in turn alter the faults state of stress playing an active role in the generation of catastrophic earthquakes[5–9].

Noble gases are powerful tools for reconstructing the birth of the Earth, its interior and the evolution over time[10–13]. Their isotopic ratios are used to investigate the dynamics of natural processes such as volcanic eruptions and earthquakes[14–18]. The lightest of the noble gases is helium (hereafter He), whose low atomic mass means that it is the only one that is able to escape into space[10]. He on Earth is present as two isotopes, $^3$He and $^4$He, with the former being mainly primordial and stored in the mantle, and the latter continuously produced by uranium (U) and thorium (Th) decay in the Earth's interior[10]. The He flux in stable continental regions is dominated by the radiogenic $^4$He that is produced in the crust (mantle He <1%)[19]. In contrast, the primordial $^3$He escapes into the atmosphere mainly from volcanoes and in regions of active tectonic (from extensive to compressive), which makes the He isotopic ratio ($^3$He/$^4$He) a powerful tool for recognizing mantle-crust tectonics in the absence of other geological evidence[4,19,20].

On the continents, groundwater acquires crustal $^4$He from the rocks that constitute the aquifer, and from the underlying crust during their circulation. Indeed, the large aquifers worldwide contribute strongly to the discharge of crustal $^4$He into atmosphere[21]. However, there is strong evidence that the continental degassing is also episodic[22], and depends on large-scale metamorphism and tectonics[23–27]. The latter degassing mechanism implies large variabilities in time and space of the crustal $^4$He outgassing to the atmosphere and also enhanced mass transfer of fluids through the crust[22,27]. It remains a challenge to quantify how the different processes occurring at depth (e.g. metamorphism, tectonics, earthquakes) sustain the release of crustal $^4$He and influence the impulsive nature of its degassing. In this scenario, identifying quantitative constraints of the volume of the fault zone at depth and the related capacity of rock underlying the impulsive degassing of $^4$He would provide powerful tools for understanding Earth degassing and the natural processes that are associated with disastrous natural events such as earthquakes.

The enhancement of rock deformation due to tectonics results in the opening and development of fractures within the crust at the grain scale. Such microscale fracturation increases as an effect of dilatation until macroscopic failures occur and the strain is released. As a consequence of the dilatancy-related microscale fracturation, crustal $^4$He stored in rocks is liberated faster from minerals and rocks[25,26,28] and it escapes towards the pore fluids and successively through the crust to the atmosphere[23]. In this framework, earthquake-related changes in volumetric strains increase the release of crustal $^4$He from rocks[27], highlighting the direct linkage between seismicity and the impulsive nature of the crustal $^4$He degassing. This evidence is augmented by rare observations of increases in the amounts of crustal $^4$He in natural fluids associated with high-magnitude earthquakes, such as the Kumamoto Earthquake in 2016 ($M = 7.3$) and the Kobe earthquake in 1995 ($M = 7.2$)[29,30].

While brittle faults are often imagined as single planar structures, in reality they should be seen as complex volumetric fault zones composed of a variety of internal structures. A fault zone can be schematically simplified in two main structural regions (Fig. 1): (1) the fault core and (2) the damage zone[31]. The fault core is referred to the volume of highly localized strain and intense shearing where most of the fault displacement is accommodated by structures as gouges, cataclasites and breccias. A damage zone is the broader volume around the fault core that exhibits second-order structures (e.g., subsidiary faults, fractures, and veins), which long-term evolution represents a key factor for strain distribution, earthquake rupture propagation, and fluid circulation through the crust. These regions represent the primary crustal volumes contributing to the enhanced release of crustal $^4$He. Its release from the rock increases with fracture development, with the $^4$He output reaching up to $10^4$ times the crustal $^4$He steady-state flux[23,32] that mainly dominates $^4$He degassing in old stable continental regions[22].

In this framework, it must be considered that both the damage zone and the fault core can host large amounts of fluids of different origins and compositions (e.g. $H_2O$, $CO_2$)[33,34], which play a fundamental role as a carrier of $^4$He that migrates through the crust. In a conceptual model (Fig. 1) where deformation and the related seismicity can result in $^4$He escaping from the minerals and rocks in which it was produced and accumulated, the fault zones thus represent (1) the zone of enhanced release of crustal $^4$He and (2) the networks of pathways through which fluids preferentially transfer crustal $^4$He through the crust towards the atmosphere (Fig. 1).

Several fieldwork and laboratory studies have investigated the volumetric changes and evolution of the fault core and damage zone due to tectonics[31,35], as well as the relationship between the nature of the damage zone and earthquake characteristics[36,37]. However, damage zone width is generally defined by studies of exhumed structures. Inconsistencies in calculation of damage zone width (e.g., due to subjectivity or ambiguity of definition and measures) makes it difficult to assess the volume of rocks at depth associated with faults where crustal $^4$He release is enhanced. Microearthquakes can revolutionize our approach to the study of crustal phenomena. In recent decades the development of dense seismic networks worldwide has generated rich, long-term earthquake catalogues, and microearthquakes can now be used as beacons for observing crustal processes down to tens of kilometres depth.

Microearthquakes indeed occur on damage zones and, hence, they allow determining the detailed structure of seismogenic fault zones at depth, to inquire about the relationships between earthquake nucleation, rock types and the presence of fluids in the fault zone[38]. The outcomes of such analyses provide new opportunities to decipher the effects of seismicity on Earth degassing and provide fundamental new insight for reconciling the dichotomy between the steady-state model and the impulsive nature of Earth degassing.

## Results and discussion

Here, we exploit the role of low magnitude earthquakes ($M < 4$) on He degassing in continental regions by computing the variability of the crustal $^4$He output over time for the seismogenic volumes of rock associated to a 12-year-long earthquake catalogue.

This study considered the Irpinia fault zone (hereafter IRPZ) in central-southern Apennine (Italy) (Fig. 2), a region affected by major deformational processes in terms of active displacements and seismogenic processes that have led to high-magnitude disastrous earthquakes (i.e. $M = 6.4$ in 1561, $M = 6.9$ in 1694, $M = 5.7$ in 1826, $M = 5.9$ in 1853, $M = 7.0$ in 1857), with the most recent being the $M = 6.9$ Irpinia earthquake in 1980[39], which occurred along NW-SE trending normal faults. This latter large event occurred as a complex rupture process involving multiple segments (mostly with dip ~60° eastward)[39]. Due to the complexity of the tectonics[40] and the occurrence of strong earthquakes, the IRPZ can be considered one of the most hazardous seismic areas in the Mediterranean region.


Content courtesy of Springer Nature, terms of use apply. Rights reserved

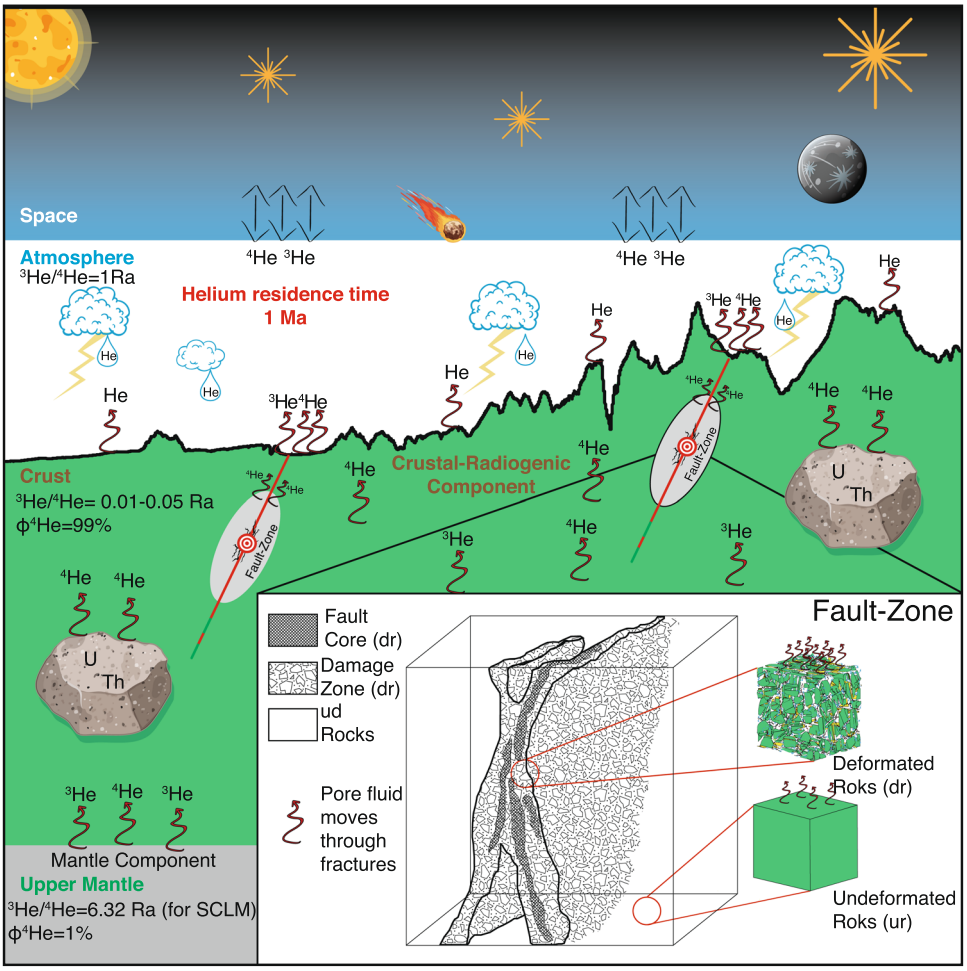


**Fig. 1 Two-dimensional sketch of earth interior below continents and the atmosphere.** Helium escapes from the continents to the atmosphere that exchanges it with space. In stable continental regions, the crustal radiogenic $^4$He dominates the output of He and the mantle component is about 1% (more details are in text). In active tectonic regions, the faults are region of enhanced porosity and permeability and they are the network of pathways through which fluids preferentially transfer to the atmosphere. Furthermore, the volumes of rocks that constitute the faults zones (damage zone plus fault core) are extensively deformed and fractured enhancing the release of crustal $^4$He because of the volumetric stress change. The insert shows a zoomed schematic representation of the fault zones as fault core plus the damage zone and the adjacent un-deformed rocks.

During the last 10 years, seismicity in the IRPZ has been monitored in real time by the Irpinia Near Fault Observatory (https://www.epos-eu.org/tcs/near-fault-observatories), which also includes the Irpinia Seismic Network (ISNet; http://isnet.fisica.unina.it). The ISNet represents a natural laboratory for studying fault evolution and rupture processes. In this study we analysed a 12-year-long earthquake catalogue (from 2008 to 2019) of distributed seismicity in an area of approximately 3700 km$^2$ (ca. 80 km × 46 km). The larger magnitude events during this 12-year-period have ranged from M = 3.4 (in 2009) to M = 4.4 (in 2012 and 2019).

The hypocentres of the present-day earthquakes appear to be spread over a large crustal volume around the fault segments that generated the M = 6.9 Irpinia earthquake in 1980, spanning depths from 2 to 20 km (Fig. 2), with a higher density of events at around 7 km and 12 km in carbonate lithology (Fig. 2).

This sector of central-southern Apennine that coincides with the IRPZ is characterized by the outgassing of volatiles of deep origin, and $CO_2$ is the dominant gaseous species[7,41,42]. Notwithstanding that the region is far from active volcanism (>70 km), the He isotopic ratio ($^3$He/$^4$He) in the high-flux $CO_2$ emissions is extremely variable, and peaks at 2.9 Ra (Ra is the $^3$He/$^4$He value in the atmosphere)[42–44]. The contribution of the air-derived He is negligible in all these gas emissions in IRPZ[42,43]. This peak value (2.9 Ra) is lower than the typical mantle He isotopic signature (6.3 Ra for subcontinental lithospheric mantle)[45] and is markedly higher than the typical crustal radiogenic signature (0.01–0.05 Ra)[46], which clearly indicates the presence of mantle-derived He in the IRPZ that is diluted by variable contributions of crust-derived $^4$He. Furthermore, high crustal radiogenic $^4$He outputs have also been computed for the IRPZ (up to $3.74 \times 10^4$ mol y$^{-1}$)[46] that cannot be explained using the steady-state model of the whole-crust production and release, the latter being up to 4 orders of magnitude lower[46]. This evidence clearly implies that tectonics control the transfer of the volatiles in this seismically active sector of central-southern Italy[42,43,46], where they play an active role in regional seismicity[8], making this region ideal for investigating the relationship between earthquakes and He degassing. Furthermore, the He isotopic signatures in natural fluids here have been constant over about 20 years of observations, indicating that the mixing of mantle-crust fluids is not perturbed during long inter-seismic period[46] (Supplementary Note 5).

At the global scale, the crustal $^4$He flux from continental regions is $3 \times 10^{10}$ atoms m$^{-2}$ s$^{-1}$, with a variability of a factor 2X[22]. We computed the year-by-year steady-state degassing in the IRPZ


Content courtesy of Springer Nature, terms of use apply. Rights reserved

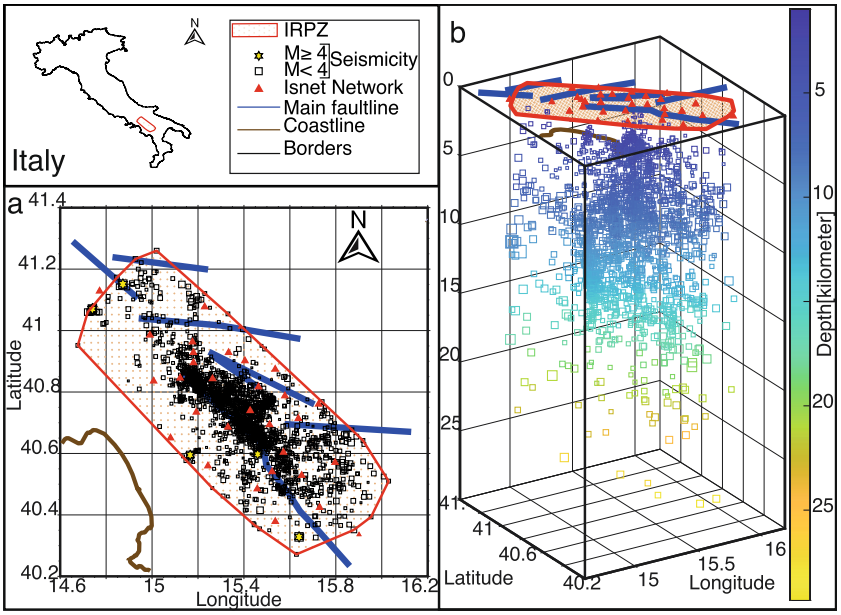


**Fig. 2 Seismic dataset recorded by ISNet seismic network in the IRPZ area (southern Italy).** Distribution of earthquakes represented in map (**a**) and in 3D (**b**) with size varying according to magnitude and coloured per hypocentral depth. Historical events with larger magnitudes (M up to 7.0; Rovida et al., 2020[54]) are represented as yellow stars. ISNet seismic stations are shown as red triangles. Normal faults from the Database of Individual Seismogenic Sources (http://diss.rm.ingv.it/diss/) are shown as blue lines. The area considered in this study is limited by a red line.

**Table 1 Abundances of U and Th (in ppm), crust thickness and density used for calculations of $^4$He production.**

| | Regional | | | Gloabal | | | Gloabal O-O | | | H | Density | |
|---|---|---|---|---|---|---|---|---|---|---|---|---|
| | U | Th | ref | U | Th | ref | U | Th/U | ref | km | g km$^{-3}$ | ref |
| Carbonates | 0.33 | 0.19 | (47) | 1.68 | 6.91 | (47) | 6.00 | 3.80 | (23) | 15.00 | $2.50{\cdot}10^{15}$ | (49) |
| Granites | 4 | 52 | (49) | | | | | | | | $2.64{\cdot}10^{15}$ | (49) |
| Gabbro | 1 | 3.5 | (49) | | | | | | | | $3.03{\cdot}10^{15}$ | (49) |
| MC | 1.6 | 6.1 | (47) | 1.3 | 6.50 | (47) | | | | 6.00 | $2.82{\cdot}10^{15}$ | (49) |
| LC | 0.29 | 3.17 | (47) | 0.6 | 3.70 | (47) | | | | 6.00 | $2.98{\cdot}10^{15}$ | (49) |

(section Whole Crust He degassing in steady-state conditions in Methods) assuming (1) U and Th contents in the rocks of the whole crust in the IRPZ of 0.3–1.6 and 0.2–6.1 ppm, respectively[47] (Table 1) and (2) a regional crustal thickness of 27 km[48]. The annual crustal steady-state $^4$He flux in the IRPZ ranges from $8.7 \times 10^9$ to $2.1 \times 10^{10}$ atoms m$^{-2}$ s$^{-1}$, where the highest value overlaps the range of the worldwide continental flux ($3 \times 10^{10}$ atoms m$^{-2}$ s$^{-1}$, with a twofold variability)[22]. The corresponding annual output from the whole crust in the IRPZ ranges from $1.2 \times 10^3$ to $4.8 \times 10^3$ mol y$^{-1}$ (Supplementary Table 3).

We also focused on faults that nucleate earthquakes in the IRPZ. We computed the volumes of both the fault cores and the damage zones of the seismogenic faults, starting from the catalogue of the earthquake source parameters obtained[34] for the ~2300 earthquakes that occurred during 2008–2019 (Supplementary Note 3 and 4 and Supplementary Data 1). The volume of the fault core (Vfc) was calculated for each event, and then the annual sum was computed (Supplementary note 3), which yielded Vfc values ranging from $4.4 \times 10^{-8}$ km$^3$ (sum of Vfc in 2008) to $1.9 \times 10^{-6}$ km$^3$ (sum of Vfc in 2019). These values are orders of magnitude lower that the annual whole-crust volume of the IRPZ (the volume that contains all the hypocentres of the annual seismicity), which ranged from $7.4 \times 10^4$ km$^3$ in 2018 to $1.2 \times 10^5$ km$^3$ in 2012 (Supplementary Fig. 1). The steady-state degassing in the core zone varies over two orders of magnitude, being between $3.9 \times 10^{-10}$ and $1.5 \times 10^{-8}$ mol y$^{-1}$ (Fig. 3). However, this is 11–13 orders of magnitudes lower than the steady-state values in the IRPZ ($1.2 \times 10^3$ to $4.8 \times 10^3$ mol y$^{-1}$; Fig. 3). Considering that the amount of $^4$He released from a deformed volume of rock is up to $10^4$ times higher than the steady-state value for the same volume of rock[23,32], even if the fault core is intensely deformed, the contribution of the fault-core crustal $^4$He to its regional degassing is still negligible, at up to $1.5 \times 10^{-4}$ mol y$^{-1}$ (Fig. 3).

In contrast, the estimated volume of the IRPZ damage zone ranges from 13.1 to $1.8 \times 10^2$ km$^3$ (Supplementary Notes 4, Supplementary Table 1), which is up to seven orders of magnitude higher than that of the fault core (Supplementary Fig. 1). The steady-state output of crustal $^4$He from the IRPZ damage zone varies from 0.1 to 0.9 mol y$^{-1}$(Supplementary Table 3), which is even lower than the regional steady-state whole-crust IRPZ degassing rate (1.2 to $2.0 \times 10^3$ mol y$^{-1}$) (Fig. 3). It is worth noting that annually there is a tenfold variability in the absence of high-magnitude earthquakes (M < 4.4), supporting the impulsive nature of crustal $^4$He degassing associated with the nucleation of earthquakes even in absence of high-magnitude earthquakes in the IRPZ. Furthermore, considering the maximum release of $^4$He from the volume of the damage zone due to rock deformation (up to $10^4$ times the steady-state release)[23,32], the annual degassing rate between 2008 and 2019 for the damage zone is up to $0.9 \times 10^4$ mol y$^{-1}$. This value is equal to or higher than the regional steady-state degassing rate from the whole non-deformed


Content courtesy of Springer Nature, terms of use apply. Rights reserved

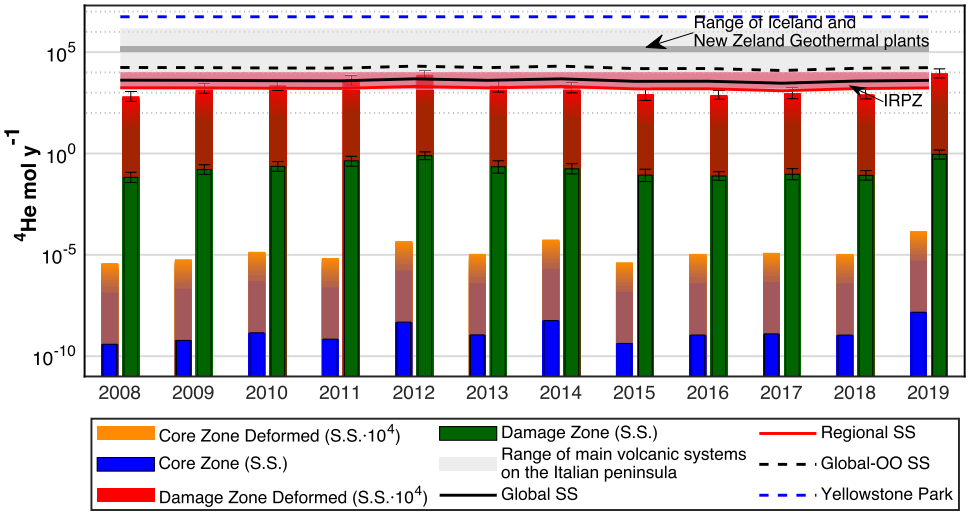


**Fig. 3 Variability of the crustal $^4$He outputs annual output (2008–2019) of the crustal $^4$He output (steady state) across the surfaces defined by earthquakes epicentres in IRPZ.** These values of the crustal $^4$He output are computed by using (1) the U and Th concentrations in the regional lithology, (2) the areas of the annual epicentres and 3) the crustal thickness below IRPZ (all the data and the equations used in the computations are in Supplementary Note 1–3). For comparison, we also computed the annual steady state output (2008–2019) of the crustal $^4$He in IRPZ by using the typical range of the U and Th concentrations in the continental crust (Table 1). The blue columns represent the steady state annual output of crustal $^4$He from the volumes of rocks that characterize the IRPZ faults cores. Here we used the U and Th concentrations of the lithology that constitute the faults cores (Table 1). The orange columns are the maximum annual output (up to $10^4$ the steady state values) from the same volume of rocks that constitute the faults cores. The green columns represent the annual steady-state output of crustal $^4$He from the IRPZ damage zones. Here we used the U and Th concentrations of the lithology that constitute the damage zones (Table 1). The red columns are the maximum annual output from the same volume of rocks that constitute the damage zones (up to $10^4$ the steady state values). The error bars represent the interquartile range (Q1–Q3), shown in the Table 2. The $^4$He output at the Yellowstone Park are from Lowenstern et al., (2014)[24]. The mantle $^4$He output the New Zealand and Iceland volcanic-related geothermal fields and the Italian volcanic systems are computed by the $CO_2$ outputs[54], the mantle C/$^3$He ratios[55], and the $^3$He/$^4$He ratio of these area[43,56–60].

crust in the IRPZ (Fig. 3). It should be noted that seismicity in the IRPZ is mainly concentrated within the limestones, which are U- and Th-poor lithology[41] (Table 1). Therefore, notwithstanding (1) a low crustal $^4$He production due to the low amount of U and Th in the seismogenic volume of rocks and (2) an absence of high-magnitude earthquakes, the degassing rate of crustal $^4$He from the seismogenic IRPZ crust, which is so high because of the intense deformation of the rock that increase the release of $^4$He from the rock, (Fig. 3) can be at least equal to that due to the whole and not-deformed IRPZ continental crust (Fig. 3).

Considering a damage zone involving U- and Th-rich rocks, such as granite and gabbro that are typical in continental regions (4 and 52 ppm U and 1 and 3.5 ppm Th)[49], and assuming a volumetric expansion of the damage zone as for the IRPZ, the output of crustal $^4$He would be up to ~$10^6$ and ~$10^5$ mol y-1, respectively (Supplementary Figs. 2 and 3). Therefore, a volume of granitic crust in a strongly deformed state can degas up to ~$10^7$ moles of crustal $^4$He over 10 years. This amount of outgassing would correspond to ~56% of the crustal $^4$He degassed during the disastrous earthquake in Kobe in 1995 ($1.8 \times 10^7$ mol)[29] and to ~1.8% of the worldwide steady-state global degassing ($5.4 \times 10^8$ mol y$^{-1}$)[29].

It is worth noting that the values of crustal $^4$He released from a damage zone in granitic rock overlap the high value of crustal $^4$He output from the large high-temperature geothermal systems worldwide (e.g. Iceland, New Zealand) and the active volcanoes of the systems of the southern of Italy (Fig. 3). However, these values are still lower than the prodigious emission of crustal $^4$He at Yellowstone National Park, where crustal metamorphism induced by a deep hotspot liberates the $^4$He that has accumulated over more than 2.5 billion years[24]. This evidence strongly reinforces the present finding that earthquake nucleation plays an active role in the impulsive nature of crustal $^4$He degassing even in the absence of high-magnitude earthquakes.

In this scenario, crustal $^4$He from the seismogenic rock volumes (Fig. 3) strongly contributes to diluting the mantle-derived He that has been recognized in worldwide regions associated with high-magnitude earthquakes (e.g. San Andreas fault, USA; southwest Japan; Anatolian fault, Turkey; Belice valley, Italy)[20,30,50–52]. According to our results, the contribution from earthquake-related crustal $^4$He varies over time and is dependent upon the extension of fault zones, their lithology and the earthquake magnitude. These findings highlight that seismicity plays an active role in the high variability of the He isotopic signature in seismic zones, and they contribute quantitatively to explaining this variability over short distances along different sectors of faults[4,20,42,52,53]. Hence, our results clearly indicate that an increase of the crustal $^4$He component over time can shift the He isotopic signature in the natural fluids released in seismic regions towards a radiogenic endmember (0.01–0.05 Ra), which is indicative of changes in the crustal stress, and hence provides hints about the preparatory phases of large earthquakes.

**Conclusions and future outlooks**. Records of sharp increases in crustal $^4$He in natural fluids due to rock microscale fracturation earthquake-related are rare, and the previous records come exclusively from high-magnitude earthquakes (e.g. that of $1.8 \times 10^7$ mol in the Kobe earthquake in 1995)[29]. Our results indicate that the background seismicity during interseismic periods also controls the impulsive degassing of crustal $^4$He. Therefore, coupling geochemical and geophysical long series of data, the crustal $^4$He outputs can be used as an indicator of the expansion of the seismogenic process, thereby making it possible to assess the volumes of deformed rocks along the faults. Our study indicates that a high frequency He monitoring is fundamental to examine and calibrate regional models capable of describing the relationship between He degassing and


Content courtesy of Springer Nature, terms of use apply. Rights reserved

**Table 2 Rate of $^4$He in deformed volumes.**

| Y | Qfc•10$^4$ | Qdz•10$^4$ | | |
|---|---|---|---|---|
| | | Median | Q1 | Q3 |
| 2008 | 3.88·10$^{-06}$ | 661.26 | 3.70·10$^{02}$ | 1.18·10$^{03}$ |
| 2009 | 6.01·10$^{-06}$ | 1612.48 | 9.33·10$^{02}$ | 2.78·10$^{03}$ |
| 2010 | 1.41·10$^{-05}$ | 2312.05 | 1.33·10$^{03}$ | 4.01·10$^{03}$ |
| 2011 | 6.94·10$^{-06}$ | 4318.01 | 2.36·10$^{03}$ | 7.30·10$^{03}$ |
| 2012 | 4.80·10$^{-05}$ | 7781.29 | 4.96·10$^{03}$ | 1.20·10$^{04}$ |
| 2013 | 1.12·10$^{-05}$ | 2218.81 | 1.08·10$^{03}$ | 4.34·10$^{03}$ |
| 2014 | 5.68·10$^{-05}$ | 1747.88 | 9.79·10$^{02}$ | 3.13·10$^{03}$ |
| 2015 | 4.27·10$^{-06}$ | 853.47 | 4.14·10$^{02}$ | 1.68·10$^{03}$ |
| 2016 | 1.11·10$^{-05}$ | 776.22 | 4.74·10$^{02}$ | 1.27·10$^{03}$ |
| 2017 | 1.26·10$^{-05}$ | 947.47 | 5.05·10$^{02}$ | 1.78·10$^{03}$ |
| 2018 | 1.10·10$^{-05}$ | 833.71 | 4.89·10$^{02}$ | 1.42·10$^{03}$ |
| 2019 | 1.47·10$^{-04}$ | 9107.57 | 5.31·10$^{03}$ | 1.49·10$^{04}$ |

Increased rate of $^4$He (mol y$^{-1}$) from deformed fault core and rock damage zone volume.

seismogenic processes at depth. Therefore, as already highlighted in volcanic surveillance[15–17], our study emphasizes the need to use new, field deployable analytical solutions that can allow He data to be acquired (amounts and isotopic signature) with a frequency from weekly to daily. These new data could help to reconstruct the temporal evolution of natural processes such as volcanic eruption and earthquakes.

This study highlights that a continuous, multidisciplinary, integrated monitoring approach that includes geochemical and geophysical observations can be the key to understanding the mechanisms underlying earthquake generation, and could facilitate to figure out premonitory rock deformation processes preceding the occurrence of a disastrous earthquake. Therefore, the novel results obtained in this study provide a new paradigm for studying the genesis of earthquakes and integrating multidisciplinary data for improving earthquake forecasts.

## Methods

**Whole crust He degassing in steady-state conditions**. On a 1-Ma timescale, the flux of $^4$He from the Earth's crust to the atmosphere is comparable to the net in situ production by alpha decay of U- and Th-series elements at the 30–40 km depth of the crust[54], suggesting that the $^4$He flux exists in the crust and eventually reaches the atmosphere with a steady flux Liu et al. (2017)[55].

The rate of $^4$He production (and release in S.S. conditions) due to α-decay of U and Th throughout the crust beneath the study area ($Q_C$ He in moles per year) is equivalent to[24]:

$$Q_{c,y} = \frac{M_{c,y}}{N_A} \cdot \alpha = \delta_c \cdot (S_{c,y} \cdot H_c) \cdot \alpha \quad (1)$$

where Mc,y is the annual mass of crust beneath the IRPZ in grams, calculated as the product of the density and volume of the crust beneath the study area, which is calculated as the product of the annual surface area (Sc,y) and the crustal thickness, and according to the local geological sections[41] this latter is given by the sum of carbonate, middle crust and lower crust thicknesses ($HC = Hc + H_{MC} + H_{LC}$). $N_A$ is the Avogadro constant and α is the crustal production of $^4$He in molgrams per year. In turn[24]

$$\alpha = \left(3.115\times 10^6 + 1.272\times 10^5\right) \cdot [U] + 7.710\times 10^5 \cdot [Th] \quad (2)$$

where [U] and [Th] are respectively the concentrations of U and Th in the crust in parts per million by weight respectively[23,24].

To compute Qc, we used literature data for the abundances of U and Th and crust thickness (Supplementary Table 3). In particular, we use three sets of U and Th concentrations for estimating the Steady-State level for area. Regarding the first and second set, we base our analysis on the U and Th amounts for a Regional Refined Reference Model and the Global Refined Reference Model proposed by Coltorti et al. (2011)[47]. For the third set (Global O-O steady state), we refer to the values proposed by O'Nions and Oxburgh 1983)[19]. Thereafter, we will refer to the result of these three configurations as the Regional, global and O-O steady-state, respectively. In addition, in the regional case, we considered granites and gabbro as alternatives in place of carbonates (see Table 1 for U and Th abundance and Supplementary Figs. 2 and 3).

**$^4$He degassing in no-steady-state conditions**. To estimate the crustal $^4$He episodic release due to seismic activity, we applied Eq. (2) to the volume related to the fault core and the damage zone (obtained from Supplementary Eq. 1 and Eq. 2 respectively), by which we obtain the rate of $^4$He release from fault core (Qfc,y) and damage zone (Qdz,y) (Supplementary Table 3). Volatile release from the rock increases as a consequence of dilatancy, and in regions affected by active tectonics the flux of $^4$He through the crust should be higher than in volume of rocks without deformation, where only a steady-state transport system is expected to act[27]. So, the release of $^4$He from rock, which is affected by dilatancy, is from 10 to 10$^4$ times higher than that in un-deformed rock[32] (i.e., of Qfc,y and Qdz,y values, see Table 2), see main text for insights.

## Data availability

The authors declare that the data supporting the findings of this study are available within the article and its Supplementary Information (see also the Methods section). The raw data (seismic waveforms) for the Irpinia Seismic Network, ISNet (i.e., FDSN code IX), are available from the Observatories and Research Facilities for European Seismology European Integrated Data Archive (URL, https://www.orfeus-eu.org/data/eida/). The ISNet seismic bulletin is available through the URL 'http://isnet-bulletin.fisica.unina.it/cgi-bin/isnet-events/isnet.cgi', while the Data-source parameters are uploaded as 'Supplementary Data 1' in the Supplementary Material.

Received: 19 March 2022; Accepted: 5 September 2022;
Published online: 03 October 2022

## References

1. Ozima, M., Korenaga, J. & Yin, Q. Z. *The Earth: Its Birth and Growth*. 1–164 (Cambridge University Press, 2012).
2. Fisher T. & Aiuppa A. AGU Centennial Grand Challenge: Volcanoes and Deep Carbon Global $CO_2$ Emissions From Subaerial Volcanism—Recent Progress and Future Challenges. *Geochem. Geophys. Geosyst.* **21**, https://doi.org/10.1029/2019GC008690 (2020).
3. Tamburello G., Pondrelli S., Chiodini G. & Rouwet, D. Global-scale control of extensional tectonics on $CO_2$ earth degassing. Nat. Commun. 4608; https://doi.org/10.1038/s41467-018-07087-z (2018).
4. Caracausi, A. & Sulli, A. Outgassing of mantle volatiles in compressional tectonic regime away from volcanism: The role of continental delamination. *Geochem. Geophys. Geosyst.* **20**. https://doi.org/10.1029/2018GC008046 (2019).
5. Miller, S. A. et al. Aftershocks driven by a high pressure $CO_2$ source at depth. *Nature* **427**, 724–727 (2004).
6. Girault, F. et al. Persistent $CO_2$ emissions and hydrothermal unrest following the 2015 earthquake in Nepal. *Nat. Commun.* **9**, 2956 (2018).
7. Di Luccio, F. et al. Seismic signature of active intrusions in mountain chains. *Sci. Adv.* **4**, 1–9 (2018).
8. Chiodini, G. et al. Carbon dioxide Earth degassing and seismogenesis in central and southern Italy. *Geophys. Res. Lett.* **31**, 2–5 (2004).
9. Chiodini, G. et al. Correlation between tectonic $CO_2$ Earth degassing and seismicity is revealed by a 10-year record in the Apennines, Italy. *Sci. Adv.* **6**, eabc2938 (2020).
10. Ozima, M. & Podosek, F. A. *Noble Gas Geochemistry*, 2nd edn, xiv 286 (Cambridge University Press, 2002) https://doi.org/10.1017/S0016756803258349.
11. Mukhopadhyay, S. Early differentiation and volatile accretion recorded in deep-mantle neon and xenon. *Nature* **486**, 101–104 (2012).
12. Caracausi, A., Avice, G., Burnard, P. G., Füri, E. & Marty, B. Chondritic xenon in the Earth's mantle. *Nature* **53**, 82–85 (2016).
13. Broadley, M. W. et al. Identification of chondritic krypton and xenon in Yellowstone gases and the timing of terrestrial volatile accretion. *Proc. Natl. Acad. Sci. USA* **117**, 13997–14004 (2020).
14. Italiano, F., Martinelli, G., Bonfanti, P. & Caracausi, A. Long-term (1997–2007) geochemical monitoring of gases from the Umbria-Marche region. *Tectonophysics* **476**, 282–296 (2009).
15. Paonita, A., Carasausi, A., Martelli, M. & Rizzo, A. Geochemical evidence for mixing between fluids exolved at different depths in the magmatic system of Mt Etna (Italy). *Geochim. Cosmochim. Acta* **84**, 380–394 (2012).
16. Paonita, A. et al. Intense overpressurization at basaltic open-conduit volcanoes as inferred by geochemical signals: the case of Mt Etna December 2018 eruption. *Sci. Adv.* **7**, eabg6297 (2021).
17. Sano, Y. et al. Helium anomalies suggest a fluid pathway from mantle to trench during the 2011 Tohoku-Oki earthquake. *Nat. Commun.* **5**, 3084 (2014).
18. Sano, Y. et al. 2015, Ten-year helium anomaly prior to the 2014 Mt Ontake eruption. *Sci. Rep.* **5**, 13069 (2013).


Content courtesy of Springer Nature, terms of use apply. Rights reserved

19. O'Nions, R. K. & Oxburg, E. H. Heat and helium in the Earth. *Nature* **306**, 429–431 (1983).
20. Boles, J. R., Garven, G., Camacho, H. & Lupton, J. E. Mantle helium along the Newport-Inglewood fault zone. *Geochem. Geophys. Geosystems.* **16**, 2364–2381 (2015).
21. Aggarwal, P. K. et al. Continental degassing of $^4$He by surficial discharge of deep groundwater. *Nat. Geosc.* **8**, 35–39 (2015).
22. Torgersen, T. Continental degassing flux of $^4$He and its variability. *Geochem. Geophys. Geosyst.* **11**, 1–15 (2010).
23. Ballentine, C. J. & Burnard, P. G. Production, release and transport of noble gases in the continental crust. *Rev. Miner. Geochem.* **47**, 481–538 (2002).
24. Lowenstern, J. B., Evans, W. C., Bergfeld, D. & Hunt, A. G. Prodigious degassing of a billion years of accumulated radiogenic helium at Yellowstone. *Nature* **506**, 355–358 (2014).
25. Bauer, S. J., Gardner, W. P. & Lee, H. Release of radiogenic noble gases as a new signal of rock deformation. *Geophys. Res. Lett.* **43**, 10,688–10,694 (2016).
26. Bauer, S. J., Gardner, W. P. & Heath, J. E. Helium release during shale deformation: experimental validation. *Geochem. Geophys. Geosystem.* **17**, 2612–2622 (2016).
27. Buttitta, D. et al. Continental degassing of helium in an active tectonic setting (northern Italy): the role of seismicity. *Sci. Rep.* **10**, 162 (2020).
28. Honda, M., Kurita, K., Hamano, Y. & Ozima, M. Experimental studies of He and Ar degassing during rock fracturing. *Earth Planet. Sci. Lett.* **59**, 429–436 (1982).
29. Sano, Y., Takahata, N., Igarashi, G., Koizumi, N. & Sturchio, N. C. Helium degassing related to the Kobe earthquake. *Chem. Geol.* **150**, 171–179 (1998).
30. Sano, Y. et al. Groundwater helium anomaly reflects strain change during the 2016 Kumamoto earthquake in Southwest Japan. *Sci. Rep.* **6**, 37939 (2016).
31. Billi, A., Salvini, F. & Storti, F. The damage zone-fault core transition in carbonate rocks: implications for fault growth, structure and permeability. *J. Struct. Geol.* **25**, 1779–1794 (2003).
32. Torgersen, T. & O'Donnell, J. The degassing flux from the solid earth: release by fracturing. *Geophys. Res. Lett.* **18**, 951–954 (1991).
33. Collettini, C. et al. Fault weakening due to $CO_2$ degassing in the Northern Apennines: short- and long-term processes. **299**, 175–194. *Geol. Soc. London Spec. Publ.* **299**, 175–194 (2008).
34. Picozzi, M. et al. Spatiotemporal evolution of microseismicity seismic source properties at the Irpinia near fault observatory, Southern Italy. *Bull. Seismol. Soc. Am* **112**, 226–242 (2021).
35. Torabi, A., Johannessen, M. U. & Ellingsen, T. S. S. Fault core thickness: insights from Siliciclastic and carbonate rocks. *Geofluids* **2019**, 2918673 (2019).
36. Jamtveit, B., Ben-Zion, Y., Renard, F. & Austrheim, H. Earthquake-induced transformation of the lower crust. *Nature* **556**, 487–491 (2018).
37. Thakur, P., Huang, Y. & Kaneko, Y. Effects of low-velocity fault damage zones on long-term earthquake behaviours on mature strike-slip faults. *J. Geophys. Res. Solid Earth* **125**, e2020JB019587 (2020).
38. Picozzi, M., Bindi, D., Zollo, A., Festa, G. & Spallarossa, D. Detecting long-lasting transients of earthquake activity on a fault system by monitoring apparent stress, ground motion and clustering. *Sci. Rep.* **9**, 16268 (2019).
39. Bernard, P. & Zollo, A. The Irpinia (Italy) 1980 earthquake: Detailed analysis of a complex normal fault. *J. Geophys. Res.* **94**, 1631–1648 (1989).
40. Adinolfi, G. M., Cesca, S., Picozzi, M., Heimann, S. & Zollo, A. Detection of weak seismic sequences based on arrival time coherence and empiric network detectability: an application at a near fault observatory. *Geophys. J. Int.* **218**, 2054–2065 (2019).
41. Improta, L., De Gori, P. & Chiarabba C. New insights into crustal structure, Cenozoic magmatism, $CO_2$ degassing, and seismogenesis in the southern Apennines and Irpinia region from local earthquake tomography. *J. Geophysic. Res-Solid Earth* **119**, https://doi.org/10.1002/2013JB010890 (2014).
42. Italiano, F., Martelli, M., Martinelli, G. & Nuccio, P. M. Geochemical evidence of melt intrusions along lithospheric faults of the southern Apennines, Italy: Geodynamic and seismogenic implications. *J. Geophys. Res.* **105**, 569–13,578 (2001).
43. Caracausi, A., Martelli, M., Nuccio, P. M., Paternoster, M. & Stuart, F. Active degassing of mantle-derived fluid: a geochemical study along the Vulture line, southern Apennines (Italy). *J. Volcanol. Geotherm. Res.* **253**, 65–74 (2013).
44. Nuccio, P. M., Caracausi, A. & Costa, M. Mantle-derived fluids discharged at the Bradanic foredeep/Apuleian foreland boundary: The Maschito geothermal gas emissions, southern Italy. *Mar. Pet. Geol.* **55**, 309–314 (2014).
45. Gautheron, C., Moreira, M. & Allègre, C. He, Ne and Ar composition of the European lithospheric mantle. *Chem. Geol.* **217**, 97–112 (2005).
46. Caracausi, A. & Paternoster, M. Radiogenic helium degassing and rock fracturing: a case study of the southern Apennines active tectonic region. *J. Geophys. Res. Solid Earth* **120**, 2200–2211 (2015).
47. Coltorti, M. et al. U and Th content in the Central Apennines continental crust: a contribution to the determination of the geo-neutrinos flux at LNGS. *Geochim. Cosmochim. Acta* **75**, 2271–2294 (2011).
48. Di Stefano R., Bianchi I., Ciaccio M.G., Carrara G. & Kissling E. (2011). Three dimensional Moho topography in Italy: new constraints from receiver functions and controlled source seismology. *Geochem. Geophys. Geosyst.* **12**, https://doi.org/10.1029/2011GC003649 (2011).
49. Schon J.H. Physical Property of Rocks, *Fundamentals and principles of petrographysics*. *Handbook* of geophysical exploration, Seismic exploration **18**, 1-583, K. Helbig and S. Treitel (Editors) (1995).
50. Doğan T. et al. Adjacent releases of mantle helium and soil $CO_2$ from active faults: Observations from the Marmara region of the North Anatolian Fault zone, Turkey. *Geochem. Geophys. Geosystem.*, **10**, https://doi.org/10.1029/2009GC002745 (2009).
51. Caracausi, A. et al. Active geodynamics of the central mediterranean sea: tensional tectonic evidences in western Sicily from mantle-derived Helium. *Geophys. Res. Lett.* **32**, L04312 (2005).
52. Kulongoski, J. T. et al. Volatile fluxes through the Big Bend section of the San Andreas Fault, California: Helium and carbon-dioxide systematics. *Chem. Geol.* **339**, 92–102 (2013).
53. Torgersen, T. Terrestrial Helium Degassing Fluxes and the Atmospheric Helium Budget: Lmplications with Respect to the Degassing Processes of Continental Crust. *Chem. Geol.* **79**, 1–14 (1989).
54. Rovida, A., Locati, M., Camassi, R., Lolli, B. & Gasperini, P. The Italian earthquake catalogue CPTI15. *Bull. Earthq. Engi.* **18**, 2953–2984 (2020).
55. Liu, W. et al. Formation time of gas reservoir constrained by the time-accumulation effect of $^4$He: case study of the puguang gas reservoir. *Chem. Geol.* **469**, 246–251 (2017).
56. Cardellini, C. et al. Monitoring diffuse volcanic degassing during volcanic unrests: the case of Campi Flegrei (Italy). *Sci. Rep.*, **7**, https://doi.org/10.1038/s41598-017-06941-2 (2017).
57. Marty, B., et al. An evaluation of the C/N ratio of the mantle from natural $CO_2$-rich gas analysis: Geochemical and cosmochemical implications. *Earth Planet. Sci. Lett.* **551**, https://doi.org/10.1016/j.epsl.2020.116574 (2020).
58. Martelli, M. et al. Helium–strontium isotope constraints on mantle evolution beneath the Roman Comagmatic Province, Italy. *Earth Planet. Sci. Lett.* **224**, 295–308 (2004).
59. Poreda, R. J. & Arnorsson, S. Helium isotopes in Iceland geothermal systems: II Helium-heat relathionships. *Geochem. Cosmochim. Acta.* **56**, 4229–4235 (1992).
60. Hulston, J. R. & Lupton, J. E. Helium isotope studies of geothermal fields in the Taupo Volcanic Zone, New Zealand. *J. Volcanol. Geotherm. Res.* **74**, 297–321 (1996).


## Acknowledgements

We would like to thank the Editor M.-L. Frezzotti and three reviewers for their comments and suggestions that allowed us to significantly improve the manuscript content and form. This research was partly carried out in the frame of the national project PRIN FLUIDS, Grant Number 20174X3P29 and the national the PON GRINT (Geoscience Research INfrastructure in iTaly) CCI:2014IT16M2OP005.

## Author contributions

A.C., D.B., M.P. (Matteo Picozzi), conceived the concepts and designed the study. M.P. (Matteo Picozzi) elaborated the geophysical data. A.C. and D.B. elaborated the geochemical data. A.C., D.B., M.P. (Matteo Picozzi), M.P. (Michele Paternoster) and T.A.S. contributed to the interpretation and discussion of the data and provided comments on and input to the manuscript. D.B. performed the Montecarlo propagation of the data. A.C. wrote the manuscript with contributions by D.B. and M.P. (Matteo Picozzi). All authors discussed the results and commented on the manuscript at all stages.

## Competing interests

The authors declare no competing interests.

## Additional information

**Supplementary information** The online version contains supplementary material available at https://doi.org/10.1038/s43247-022-00549-9.

**Correspondence** and requests for materials should be addressed to Antonio Caracausi.

**Peer review information** *Communications Earth & Environment* thanks Francesco Frondini and the other, anonymous, reviewer(s) for their contribution to the peer review of this work. Primary Handling Editors: Maria Luce Frezzotti, Joe Aslin. Peer reviewer reports are available.

**Reprints and permission information** is available at http://www.nature.com/reprints

**Publisher's note** Springer Nature remains neutral with regard to jurisdictional claims in published maps and institutional affiliations.



Content courtesy of Springer Nature, terms of use apply. Rights reserved

**Open Access** This article is licensed under a Creative Commons Attribution 4.0 International License, which permits use, sharing, adaptation, distribution and reproduction in any medium or format, as long as you give appropriate credit to the original author(s) and the source, provide a link to the Creative Commons license, and indicate if changes were made. The images or other third party material in this article are included in the article's Creative Commons license, unless indicated otherwise in a credit line to the material. If material is not included in the article's Creative Commons license and your intended use is not permitted by statutory regulation or exceeds the permitted use, you will need to obtain permission directly from the copyright holder. To view a copy of this license, visit http://creativecommons.org/licenses/by/4.0/.

© The Author(s) 2022



Content courtesy of Springer Nature, terms of use apply. Rights reserved

# Terms and Conditions

Springer Nature journal content, brought to you courtesy of Springer Nature Customer Service Center GmbH (“Springer Nature”).
Springer Nature supports a reasonable amount of sharing of research papers by authors, subscribers and authorised users (“Users”), for small-scale personal, non-commercial use provided that all copyright, trade and service marks and other proprietary notices are maintained. By accessing, sharing, receiving or otherwise using the Springer Nature journal content you agree to these terms of use (“Terms”). For these purposes, Springer Nature considers academic use (by researchers and students) to be non-commercial.
These Terms are supplementary and will apply in addition to any applicable website terms and conditions, a relevant site licence or a personal subscription. These Terms will prevail over any conflict or ambiguity with regards to the relevant terms, a site licence or a personal subscription (to the extent of the conflict or ambiguity only). For Creative Commons-licensed articles, the terms of the Creative Commons license used will apply.
We collect and use personal data to provide access to the Springer Nature journal content. We may also use these personal data internally within ResearchGate and Springer Nature and as agreed share it, in an anonymised way, for purposes of tracking, analysis and reporting. We will not otherwise disclose your personal data outside the ResearchGate or the Springer Nature group of companies unless we have your permission as detailed in the Privacy Policy.
While Users may use the Springer Nature journal content for small scale, personal non-commercial use, it is important to note that Users may not:

1. use such content for the purpose of providing other users with access on a regular or large scale basis or as a means to circumvent access control;
2. use such content where to do so would be considered a criminal or statutory offence in any jurisdiction, or gives rise to civil liability, or is otherwise unlawful;
3. falsely or misleadingly imply or suggest endorsement, approval , sponsorship, or association unless explicitly agreed to by Springer Nature in writing;
4. use bots or other automated methods to access the content or redirect messages
5. override any security feature or exclusionary protocol; or
6. share the content in order to create substitute for Springer Nature products or services or a systematic database of Springer Nature journal content.

In line with the restriction against commercial use, Springer Nature does not permit the creation of a product or service that creates revenue, royalties, rent or income from our content or its inclusion as part of a paid for service or for other commercial gain. Springer Nature journal content cannot be used for inter-library loans and librarians may not upload Springer Nature journal content on a large scale into their, or any other, institutional repository.
These terms of use are reviewed regularly and may be amended at any time. Springer Nature is not obligated to publish any information or content on this website and may remove it or features or functionality at our sole discretion, at any time with or without notice. Springer Nature may revoke this licence to you at any time and remove access to any copies of the Springer Nature journal content which have been saved.
To the fullest extent permitted by law, Springer Nature makes no warranties, representations or guarantees to Users, either express or implied with respect to the Springer nature journal content and all parties disclaim and waive any implied warranties or warranties imposed by law, including merchantability or fitness for any particular purpose.
Please note that these rights do not automatically extend to content, data or other material published by Springer Nature that may be licensed from third parties.
If you would like to use or distribute our Springer Nature journal content to a wider audience or on a regular basis or in any other manner not expressly permitted by these Terms, please contact Springer Nature at

onlineservice@springernature.com